SRTTU

JCARME
ISSN: 2228-7922

Journal of Computational and Applied Research
in Mechanical Engineering
Vol. 2, No. 1, pp. 15-24, Sept. 2012
http://jcarme.srttu.edu

Effect of shell axial deformation on flutter of cantilevered cylindrical shells under follower forces

Mohammad Ebrahim Torki Harchegani* **and Mohammad Taghi Kazemi**

Department of Civil Engineering, Sharif University of Technology, Tehran, Islamic Republic of Iran, zip code: 1136511155.

Article info:
Received: 18/11/2011
Accepted: 04/04/2012
Online: 11/09/2012

Keywords:
Axial follower force,
Flutter,
Cantilevered
cylindrical shell,
Circumferential
mode number

Abstract

Axial vibration effect of shell particles on dynamic stability of a cantilevered cylindrical shell under an axial follower force was addressed. In spite of free-ended shells, the reduced axial force under this effect cannot be derived analytically. Instead, an approximate method was proposed based on the fact that the static (and harmonic) axial deformation under an axial load in a free-ended beam are (almost) zero in a particular point near the middle of the beam, which was adopted as the equivalent fixed end of a cantilever. The work done by the nonconservative follower force was derived for a cantilevered beam and was extended to the case of a cantilevered cylindrical shell. The flutter load for a long free-ended shell was calculated using the equivalent cantilevered half-shell and compared with the previous results. Then, flutter load was calculated with and without the axial vibration effect for cantilevered shells with different lengths and thicknesses and the effect of each parameter was assessed on the flutter load and the critical circumferential mode number in each case.

Nomenclature

A	Cross sectional area of the shell
A_{ij}	Zero'th-order integral of Q_{ij} with respect to thickness
B_{ij}	First-order integral of Q_{ij} with respect to thickness
D_{ij}	Second-order integral of Q_{ij} with respect to thickness
E	Elasticity modulus
h	Shell thickness
I	Beam area moment of inertia
I_i	Shell i'th order rotary inertia
K	Kinetic energy of the system
K_s	Shear correction factor
L	Length of the shell
M	Axial stress moment resultant per unit length of the shell cross section circumference
n	Number of circumferential waves on the shell
N	Axial stress resultant per unit length of the shell cross section circumference
P	Resultant concentrated follower load
Q	Transverse (normal to thickness) shear stress resultant per unit length of the shell cross section circumference
S_{ij}	Stiffness coefficients used in the *ABD* matrix
R	Shell radius
t	Time duration (*sec*)
u	Displacement along x axis
v	Displacement along θ axis
w	Displacement along z axis

*Corresponding author.
Email address: mohamad_torky@yahoo.com

u_0	Displacement of the middle surface along x axis
v_0	Displacement of the middle surface along θ axis
w_0	Displacement of the middle surface along z axis
U	Strain energy stored in the system
V	Potential of the conservative external forces
x	Coordinate along the shell generating axis
z	Coordinate along the shell thickness
β_b	Beam non-dimensional load parameter
β_{bcr}	Critical beam non-dimensional load parameter
β_s	Shell non-dimensional load parameter
β_{scr}	Critical shell non-dimensional load parameter
ε_i^j	Translational strain component
φ_x	Change of slope of the normal to the middle surface around θ axis
φ_θ	Change of slope of the normal to the middle surface around x axis
ψ_j^i	Weight function used in Galerkin method
μ	Mass per unit length
υ	Poisson's ratio
Ω_b	Beam non-dimensional frequency parameter
ω	Natural frequency (eigenvalue of the equivalent equation system)
ω_i^j	Rotational strain component
ρ	Mass density
θ	Circumferential coordinate

1. Introduction

The flutter problem dates back to 1969 in the cantilever rubber pipes containing low-pressure air flows. Two basic types of instability may exist in the pipes containing fluid flows: one characterized with zero frequency called divergence, and the other with very high frequency approaching infinity known as flutter. However, the prevailing instability type in these structures is flutter, which occurs in high-speed fluid flows [1]. When undergoing follower forces, the only instability type in the structures with moderate thickness is flutter, which is, for the most part, limited to columns, reservoirs,and aero-space structures, especially projectiles such as missiles [2].

The most well-known follower loading in practice is Beck's problem, in which a concentrated follower force is applied at the free end of a cantilever. Practical applications of this problem include the thrust applied on the end of a projectile or missile by a rocket, the thrust applied on the body of aircraft structures by a jet engine, gas turbine rotors, the gripping force in disk brakes, the eccentric load exerted on a platform by a tip mass, etc. [3–5].

A large cache of work concerning flutter problem of plates and shells has been reported in the literature. Altman and De Oliviera studied the dynamic stability of cantilever cylindrical and conical panels with and without slight internal damping. They asserted that, due to numerical defects, the calculated critical load becomes occasionally very small. To overcome this problem, a slight damping matrix proportional to the stiffness matrix can be used in the solution [6 and 7].

Dynamic stability of thin cylindrical panels with different boundary conditions under concentrated and distributed follower forces was first studied by Bismark Nasr using the finite element method with C^1 continuity [8]. He considered concentrated and distributed loading both separately and simultaneously and calculated the flutter load in each case in terms of radius, panel arch angle and thickness. Considering the effect of axial vibration, the dynamic stability of free-free cylindrical shells under axial follower forces was studied by Park and Kim [2], who used the finite element method with the First-order Shear Theory (FST) and concluded that FST was valid only for $L/R>20$ and for $L/R>40$. The cylindrical shell can be analyzed with the beam theory in certain regions of h/R. The same problem for cylindrical shells was studied considering the fluid-shell interaction by Jung et al., who concluded that, in most cases except those with very low filling ratios, the presence of liquid in the cylinder increased stability [9].

To the best knowledge of the authors, work on the effect of axial vibration of the shell on the dynamic stability (flutter) of cylindrical shells has been reported only for the free-free boundary condition. Thus, in the present research, the so-called effect was solved for the clamped-free (cantilevered) condition, which has not been accounted for in the literature. At first, flutter loads were calculated for different L/R and h/R ratios. Then, tables containing the effect of axial vibration on numbers of critical circumferential mode and flutter loads were collected for different L/R and h/R ratios.

2. Formulation

Consider a cylindrical shell with radius R, thickness h and length L. In case the coordinate system is considered as shown in Fig. 1(a), then, FST can be used to write the deformation components of any point as [10]:

$$\begin{aligned} u(x,\theta,z,t) &= u_0(x,\theta,t) + z\,\varphi_x(x,\theta,t) \\ v(x,\theta,z,t) &= v_0(x,\theta,t) + z\,\varphi_\theta(x,\theta,t) \\ w(x,\theta,z,t) &= w_0(x,\theta,t) \end{aligned} \quad (1)$$

where u_0, v_0 and w_0 are the displacement components of the middle surface and φ_x and φ_θ are changes in the slope of the normal to the middle surface around θ and x axes, respectively. The stress resultants per unit length for a cylindrical shell are shown in Fig. 1(b).

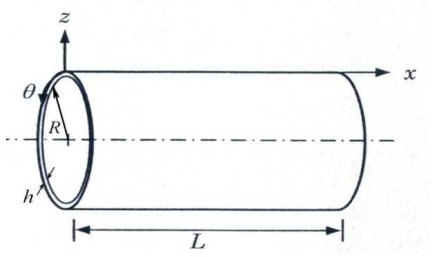

(a)

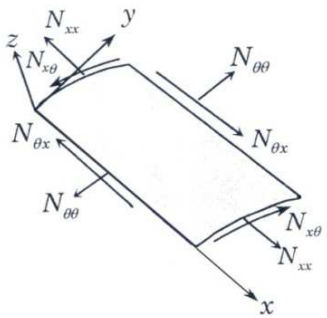

(b)

Fig. 1. (a) The coordinate system, (b) strain resultants considered for cylindrical shells.

For the strain components, Love's hypotheses were used, in which the transverse normal was inextensible, the normals to the reference surface of the shell before deformation remained straight, but not necessarily normal, after deformation, deflections and strains were infinitesimal and the transverse normal stress was negligible, i.e. plane-stress state was invoked [10].

Using Eq. (1) and considering Love's above-mentioned hypotheses, the strain tensor elements can be written as follows [10]:

$$\begin{aligned} &\varepsilon_1 = \varepsilon_1^0 + z\varepsilon_1^1,\ \varepsilon_2 = \frac{1}{1+z/R}\left(\varepsilon_2^0 + z\varepsilon_2^1\right) \\ &\varepsilon_6 = \omega_1^0 + z\omega_1^1 + \frac{1}{1+z/R}\left(\omega_2^0 + z\omega_2^1\right) \\ &\varepsilon_4 = \frac{1}{1+z/R}\varepsilon_4^0,\ \varepsilon_5 = \varepsilon_4 \end{aligned} \quad (2)$$

in which the superscripted components are defined as:

$$\begin{aligned} &\varepsilon_1^0 = \frac{\partial u_0}{\partial x},\ \varepsilon_2^0 \\ &= \frac{1}{R}\left(\frac{1}{R}\frac{\partial v_0}{\partial\theta} + \frac{\partial R}{\partial x}u_0 + w_0\right) \\ &\varepsilon_4^0 = \frac{1}{R}\left(\frac{1}{R}\frac{\partial w_0}{\partial\theta} + R\varphi_\theta - v_0\right), \\ &\varepsilon_5^0 = \frac{\partial w_0}{\partial x} + \varphi_x \\ &\omega_1^0 = \frac{\partial v_0}{\partial x},\ \omega_2^0 = \frac{1}{R^2}\frac{\partial u_0}{\partial\theta} \\ &\varepsilon_1^1 = \frac{\partial\varphi_x}{\partial x},\ \varepsilon_2^1 = \frac{1}{R^2}\frac{\partial\varphi_\theta}{\partial\theta} \\ &\omega_1^1 = \frac{\partial\varphi_\theta}{\partial x},\ \omega_2^1 = \frac{1}{R^2}\frac{\partial\varphi_x}{\partial\theta} \end{aligned} \quad (3)$$

The stress resultants vectors in unit length (of the shell circumference), N, M and Q can be obtained in terms of strain components using the ABD matrix as stated in Eq. (4), in which stiffness factors are defined in Eq. (5) [10].

$$\begin{bmatrix}\{N\}\\ \{M\}\end{bmatrix}=\begin{bmatrix}[A] & [B]\\ [B] & [D]\end{bmatrix}\begin{bmatrix}\{\varepsilon^0\}\\ \{\varepsilon^1\}\end{bmatrix}$$

$$\begin{Bmatrix}Q_2\\ Q_1\end{Bmatrix}=K_s\begin{bmatrix}A_{44} & A_{45}\\ A_{45} & A_{55}\end{bmatrix}\begin{Bmatrix}\varepsilon_4^0\\ \varepsilon_5^0\end{Bmatrix} \quad (4)$$

$$\{\varepsilon^0\}=\begin{Bmatrix}\varepsilon_1^0\\ \varepsilon_2^0\\ \varepsilon_6^0\end{Bmatrix},\ \{\varepsilon^1\}=\begin{Bmatrix}\varepsilon_1^1\\ \varepsilon_2^1\\ \varepsilon_6^1\end{Bmatrix}$$

$$\varepsilon_6^0=\omega_1^0+\omega_2^0,\ \varepsilon_6^1=\omega_1^1+\omega_2^1$$

$$\left(A_{ij},B_{ij},D_{ij}\right)=\int_{-h/2}^{h/2}S_{ij}(z)\left(1,z,z^2\right)dz,\ i,j=1,$$

$$A_{ij}=\int_{-h/2}^{h/2}S_{ij}(z)dz,\ i,j=4,5$$

$$S_{11}=S_{22}=\frac{E}{1-\upsilon^2},\ S_{12}=S_{21}=\frac{\upsilon E}{1-\upsilon^2} \quad (5)$$

$$S_{44}=S_{55}=S_{66}=\frac{E}{2(1+\upsilon)}$$

where K_s is the shear correction factor, which is $\pi^2/12$ for cylindrical shells [2], and υ is Poisson's ratio, which was taken as 0.3 (for stainless steel) in this research.

In order to derive the governing equations of motion, Hamilton's principle was used as [10]:

$$\int_0^T\left[\delta K-\delta U+\delta W_{nc}\right]dt=0 \quad (6)$$

where δK and δU are variations of kinetic and strain energy, respectively, defined as:

$$\delta K=\int_0^L\int_0^{2\pi}\begin{bmatrix}I_0\left(\dot{u}_0\ \delta\dot{u}_0+\dot{v}_0\ \delta\dot{v}_0+\dot{w}_0\ \delta\dot{w}_0\right)\\ +I_1\left(\dot{\phi}_x\ \delta\dot{u}_0+\dot{u}_0\ \delta\dot{\phi}_x+\dot{\phi}_\theta\ \delta\dot{v}_0+\dot{v}_0\ \delta\ \dot{\phi}_\theta\right)\\ +I_2\left(\dot{\phi}_x\delta\ \dot{\phi}_x+\dot{\phi}_\theta\ \delta\ \dot{\phi}_\theta\right)\end{bmatrix}Rdxd\theta$$

$$\delta U=\int_0^L\int_0^{2\pi}\begin{bmatrix}N_x\delta\ \varepsilon_1^0+M_x\delta\ \varepsilon_1^1+N_\theta\delta\ \varepsilon_2^0+M_\theta\delta\ \varepsilon_2^1\\ +\left(N_{x\ \theta}\delta\ \omega_1^0+N_{\theta\ x}\delta\ \omega_2^0\right)\\ +\left(M_{x\ \theta}\delta\ \omega_1^1+M_{\theta\ x}\delta\ \omega_2^1\right)\\ +Q_{\ \theta}\delta\ \varepsilon_4^0+Q_x\delta\ \varepsilon_5^0\end{bmatrix}Rdxd\theta$$

$$I_i=\int_{-h/2}^{h/2}\rho(z)\left(1+\frac{z}{R}\right)(z)^i dz,\ (i=0,1,2) \quad (7)$$

where the dot superscript shows differentiation with respect to time and δW_{nc} is variation of the work done by nonconservative forces. The effect of axial vibration on the internal axial load can be derived by differentiating the static part of the axial displacement under an axial load with respect to x, which gives the equivalent axial strain, and multiplying this equivalent strain by EA, in which E is the elasticity modulus and A is the cross section area. For instance, the axial displacement of a free-free beam is [11]:

$$u(x,t)=\frac{P}{2m\ell}t^2+\frac{P}{EA\ell}\left[\frac{(\ell-x)^2}{2}-\frac{\ell^2}{6}\right]$$
$$-\frac{2P\ell}{\pi^2EA}\sum_{n=1}^{\infty}\left(\frac{1}{n^2}\cos\frac{n\pi x}{\ell}\cos\omega_n t\right),\ \omega_n=n\pi\sqrt{\frac{EA}{m\ell^2}} \quad (8)$$

where the first term is the rigid-body displacement, the second term is the static part and the third term is the harmonic part of the displacement. Thus, the effect of axial vibration on the internal axial load of such a beam is obtained as follows [11]:

$$P(x)=EA\times\frac{P}{EA\ell}\frac{\partial}{\partial x}\left[\frac{(\ell-x)^2}{2}-\frac{\ell^2}{6}\right]$$
$$=-P\left(1-\frac{x}{\ell}\right) \quad (9)$$

This $P(x)$ ought to be used in the domain portion of the equation for calculating δW_{nc}. However, for a cantilevered beam, it is not possible to derive the static part of the axial vibration under an axial load as a function of x. Instead, in case the sum of the static and dynamic parts of $u(x,t)$ is plotted against x at different instants of time, then, it can be observed that, in $x=\ell\left(1-1/\sqrt{3}\right)$, almost for all times, this sum is, if not exactly, very close to zero (as demonstrated in Fig. 2). This point was obtained by calculating the point at which the static part of the displacement became zero.

Thus, it can be inferred that the portion of the free-free beam from $x = \ell\left(1-1/\sqrt{3}\right)$ to the end can be idealized as a cantilevered beam since the point $x = \ell\left(1-1/\sqrt{3}\right)$ is almost the zero point of the axial displacement almost at every instant. Therefore, the modified equation of the static displacement could be extracted by changing the variables as depicted in Fig. 3 and stated in Eq. (10).

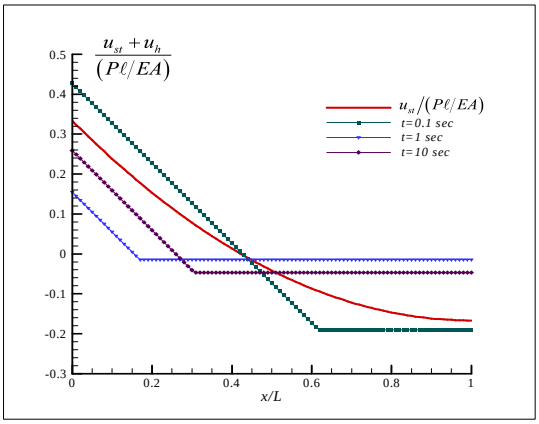

Fig. 2. The sum of the static and harmonic portions of axial displacement under an axial load at different instants.

$$X = x - \frac{\ell}{\sqrt{3}} \Rightarrow x = X + \frac{\ell}{\sqrt{3}}$$
$$U_{st} = u_{st} \Rightarrow u_{st} = U_{st} \qquad (10)$$

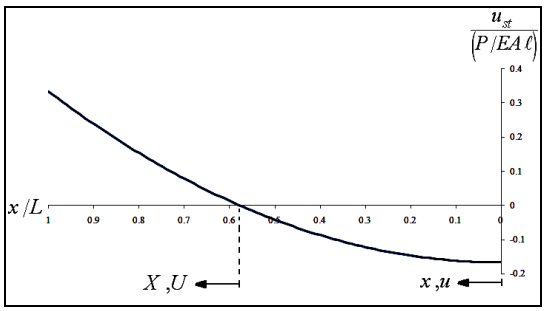

Fig. 3. Changing the displacement origin to obtain the cantilevered beam displacement from that of a free-free beam.

Thus, the modified static displacement for the cantilevered beam can be written as:

$$U_{st} = -\frac{P}{EA\ell}\left[\frac{1}{2}\left(X + \frac{\ell}{\sqrt{3}}\right)^2 - \frac{\ell^2}{6}\right]$$
$$\Rightarrow P(X) = EA\frac{\partial U_{st}}{\partial X} = -P\left(\frac{X}{\ell} + \frac{1}{\sqrt{3}}\right) \qquad (11)$$
$$= -P\left[\frac{X}{L}\left(1-\frac{1}{\sqrt{3}}\right) + \frac{1}{\sqrt{3}}\right]$$

Thus, the work done by the nonconservative force in a cantilevered beam with the exertion of integration by parts could be written as:

$$\delta w_{nc} = \int_0^1 P(x)\frac{\partial v}{\partial x}\frac{\partial \delta v}{\partial x}dx - P\left(\frac{\partial v}{\partial x}\delta v\right)_{x=1}$$
$$\int_0^1 P(x)\frac{\partial v}{\partial x}\frac{\partial \delta v}{\partial x}dx = \left[P(x)\frac{\partial v}{\partial x}\delta v\right]_0^1$$
$$-\delta v\int_0^1 \frac{\partial}{\partial x}\left(P(x)\frac{\partial v}{\partial x}\right)dx \qquad (12)$$
$$= P\left(\frac{\partial v}{\partial x}\delta v\right)_{x=1} - \delta v\int_0^1 \frac{\partial}{\partial x}\left(P(x)\frac{\partial v}{\partial x}\right)dx$$
$$\Rightarrow \delta w_{nc} = -\left[\int_0^1\left(P'(x)\frac{\partial v}{\partial x} + P(x)\frac{\partial^2 v}{\partial x^2}\right)dx\right]\delta v$$

Similarly, the formula for a cantilevered cylindrical shell can be generalized as:

$$\delta w_{nc} = -\left[\int_0^1\left(\bar{P}'(x)\frac{\partial v}{\partial x} + \bar{P}(x)\frac{\partial^2 v}{\partial x^2}\right)dx\right]\delta v$$
$$-\left[\int_0^1\left(\bar{P}'(x)\frac{\partial w}{\partial x} + \bar{P}(x)\frac{\partial^2 w}{\partial x^2}\right)dx\right]\delta w \qquad (13)$$

where $\bar{P} = P/2\pi R$ is the force per unit length of the shell circumference, on the premise that the axial stress is uniformly distributed along the thickness. Figure 4 includes the scheme of Beck's follower loading.

After replacing the stress resultants by their strain equivalents from Eq. (6) and replacing strain components in terms of deformations from Eq. (2), the following differential operators will be derived:

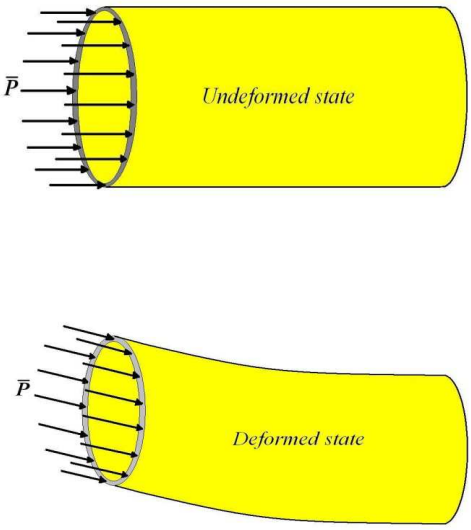

Fig. 4. Schematic shape of follower loading in Beck's problem.

$$\int_{t_1}^{t_2}\int_{0}^{2\pi}\left(\int_{0}^{L}[L]\{\Delta\}dx+\left[[L']\{\Delta\}\right]_0^L\right)Rd\theta dt=\{0\}$$
$$\{\Delta\}=\{u_0,v_0,w_0,\phi_x,\phi_\theta\}^T \qquad (14)$$

where L and L' matrices are differential operators of the domain and boundary, respectively, the elements of which are defined in Appendix A. It can be easily proven that all of the equations were orthogonal in terms of θ if the displacements were defined using alternative sine and cosine functions as stated in Eq. (15). Thus, e base functions and mode shape functions can be chosen as follows [2 and 10]:

$$\begin{aligned}
u_0 &= \sum_{j=1}^{q} U_j(x)\cos(n\theta)e^{\omega t}\\
v_0 &= \sum_{j=1}^{q} V_j(x)\sin(n\theta)e^{\omega t}\\
w_0 &= \sum_{j=1}^{q} W_j(x)\cos(n\theta)e^{\omega t}\\
\varphi_x &= \sum_{j=1}^{q} X_j(x)\cos(n\theta)e^{\omega t}\\
\varphi_\theta &= \sum_{j=1}^{q} Y_j(x)\sin(n\theta)e^{\omega t}
\end{aligned} \qquad (15)$$

where each base function can be defined as an unknown coefficient multiplied by the corresponding shape function. The superscripts denoting functions corresponding to u_0, …, and φ_θ, and a^i_j (i = 1 . . . 5) are the unknown coefficients that could be determined by exerting any approximation method such as Galerkin's method. For the mode shape functions, $\psi^i_j(x)$ (i = 1 . . . 5) which satisfy essential boundary conditions of the cantilevered cylinder, the following polynomials were considered [6]:

$$\begin{aligned}
&U_j(x)=a^1_j\psi^1_j(x),\ V_j(x)=a^2_j\psi^2_j(x)\\
&W_j(x)=a^3_j\psi^3_j(x),\ X_j(x)=a^4_j\psi^4_j(x)\\
&Y_j(x)=a^5_j\psi^5_j(x)\\
&\psi^1_j=\psi^2_j=x^j,\ \psi^3_j=x^{j+1}\\
&\psi^4_j=\frac{d\psi^3_j}{dx},\ \psi^5_j=\psi^3_j
\end{aligned} \qquad (16)$$

After applying Galerkin's method, stiffness and mass matrices can be defined as functions of n. The stiffness matrix was also a function of $\bar{P}$. The equations obtained by the application of the so-called generalized Galerkin method were algebraic equations in terms of a^i_j (i = 1 . . . 5). By setting the determinant of the coefficient matrix to zero to impose the condition of non-trivial solution, as stated in Eq. (17), ω will be obtained:

$$\det\left(\boldsymbol{K}_{(\bar{P},n)}+\omega^2\boldsymbol{M}_{(n)}\right)=0 \qquad (17)$$

ω is a complex number with a zero real part until the shell loses its stability under the applied follower forces. As soon as instability occurs, the real part begins to become positive or negative. In order to facilitate verification for future works, the non-dimensional load parameter β_s for the shell model can be considered as the comparator, as defined in the following way [2]:

$$\beta_s=\frac{1-\upsilon^2}{Eh}\bar{P} \qquad (18)$$

3. Results and discussion

Calculations in the present study demonstrated that the optimum number of terms needed for convergence in the Galerkin method was 6, as was confirmed in [6]. Subsections 3.1 and 3.2 presented verification of results with previous works. When the imaginary part of the natural frequency (ω) of two sequential modes became zero and the real part got greater than zero, divergence occurred. Alternatively, when the imaginary part of the natural frequency of two sequential modes became equal and the real part got greater than zero, flutter occurred. The results demonstrated that instability under follower forces could be flutter or divergence. However, flutter always took place before divergence.

3. 1. Flutter of very long shells (Equivalent beam model)

In order to verify the present computational approach, the problem was first solved for long shells and the results were compared with those obtained with the beam model. The non-dimensional load and frequency parameters in the beam model were defined in the literature as [5]:

$$\beta_b = \frac{PL^2}{EI}, \Omega_b = \omega L^2 \sqrt{\frac{\mu}{EI}} \tag{19}$$

where μ is the mass per unit length ($\mu = 2\pi Rh\rho$). In order to analyze very long shells with the equivalent beam model, the following identity can be used:

$$A = 2\pi Rh, I = \pi R^3 h \Rightarrow \frac{I}{AL^2} = \frac{1}{2}\left(\frac{R}{L}\right)^2$$
$$\Rightarrow \beta_b = \frac{2(L/R)^2}{1-\upsilon^2}\beta_s \tag{20}$$

Figure 5 shows the results for Beck's problem.

3. 2. Flutter load of a free-free cylindrical shell due to an axial follower load

For considering the effect of axial vibration of the shell on the flutter load of cylindrical shells, no results were found to verify the results, except those obtained by Park and Kim [2]. Since a free-free beam (or shell) can be idealized with a cantilevered beam (or shell) with half of the actual length only when it is long, the considered shell for validating the present results had the following properties:

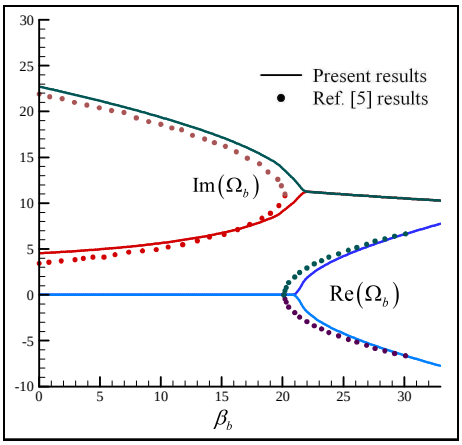

Fig. 5. Changing of the imaginary and real parts of Ω_b vs. β_b for Beck's problem.

$$E = 2\times10^{11}\,\mathrm{Pa}, L/R = 80, h/R = 0.1, n = 1.$$

Since flutter occurred between the third and fourth modes (i.e. between the first and the second flexural modes) in the free-free shell described above, the imaginary parts of the third and fourth modes were compared with those of the first and second modes in the equivalent cantilevered model with half of the free-free shell and, as indicated in Fig. 6, the results were in good agreement.

3. 3. Effect of axial vibration on flutter of cantilevered cylindrical shells

The results in this section include the effect of axial vibration on the critical circumferential mode number and the critical (flutter) load. The results were developed for stainless steel with the elasticity modulus of 2.07788×10^{11} Pa for different *h/R* and *L/R* ratios.

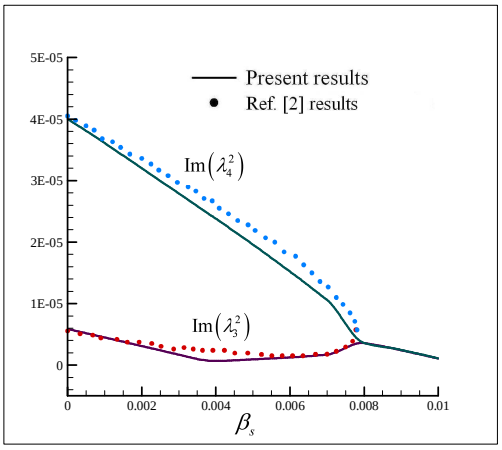

Fig. 6. Comparison between the frequencies of the first and second flexural modes of a long free-free shell with those of the idealized half-length cantilevered shell, considering the effect of axial vibration of the shell.

3. 3. 1. Effect on the critical circumferential mode number

The effect of axial vibration on the critical circumferential mode number (n_{cr}) is illustrated in Table 1. It can be observed that the combined effect n_{cr} was, in all cases, less or equal to n_{cr} of ordinary Beck's problem. However, this effect did not influence n_{cr} remarkably.

3. 3. 2. Effects on the flutter load

The effect of axial vibration on the flutter load is demonstrated in Table 2 for different h/R and L/R ratios, where η_C is the ratio of the combined-effect flutter load to the ordinary Beck's flutter load.

As can be observed in the above table, the axial vibration of the shell increased the flutter load to a limited extent. Neglecting this effect overestimated the flutter load. It can be also observed that η_C reduced with *L/R* for a specified *h/R*. Thus, it can be inferred that the axial vibration effect was more significant in shorter shells. Moreover, as the shell became very long and moderately thick, i.e. in beam-like ranges, η_C became almost constantly equal to 1.17 for all lengths and thicknesses.

4. Conclusions

In the present paper, the axial vibration effect on the dynamic stability of cantilevered circular cylindrical shells was investigated under axial follower (Beck's) loading. To do so, flutter loads and critical circumferential mode numbers (corresponding to the minimum flutter load) were calculated for different thickness and length ratios using the extended Galerkin method; the results were in good agreement with those of previous ones. Then, the effect of axial vibration on the critical circumferential mode number and flutter load was demonstrated in tables, which demonstrated that the combined-effect circumferential mode number was less or equal to that of ordinary Beck's loading. However, this phenomenon did not have a great effect on the circumferential mode number. Also, the flutter load increased with the axial vibration effect. However, this effect was more significant in short shells rather than longer ones. The axial vibration effect was constant for every thickness and length in long-thick, i.e. beam-like shells.

References

[1] Z. Elfesoufi and L. Azrar, “Buckling, Flutter and Vibration Analysis of Beams by Integral Equation Formulations”, *Journal of Computers and Structures*, Vol. 83, pp. 2632–2649, (2005).

[2] S. H. Park and J. H. Kim, “Dynamic Stability of a Completely Free Circular Cylindrical Shell Subjected to a Follower Force”, *Journal of Sound and Vibration*, Vol. 231, No. 4, pp. 989–1005, (2000).

[3] T. E. Simkins and G. L. Anderson, “Stability of Beck's Column Considering Support Characteristics”, *Journal of Sound and Vibration*, Vol. 39, No. 3, pp. 359–369, (1975).

[4] A. P. Seyranian and I. Elishakoff, *Modern problems of structural stability*, *International Centre for Mechanical Sciences*, Springer-Verlag, Wien, New York, (2002).

[5] G. J. Simitses and D. H. Hodges, *Fundamentals of Structural Stability*, Elsevier, Burlington, (2006).

[6] W. Altman and M. G. De Oliviera, "Vibration and Stability of Cantilevered Cylindrical Shell Panels under Follower Forces", *Journal of Sound and Vibration*, Vol. 122, No. 2, pp. 291–298, (1988).

[7] W. Altman and M. G. De Oliviera, "Vibration and Stability of Shell Panels with Slight Internal Damping under Follower Forces", *Journal of Sound and Vibration*, Vol. 136, No. l, pp. 45–50, (1990).

[8] M. N. Bismarck Nasr, "Dynamic Stability of Shallow Shells Subjected to Follower Forces", *AIAA Journal*, Vol. 33, No. 2, pp. 355–360, (1995).

[9] S. W. Jung, K. S. Na, and J. H. Kim, "Dynamic Stability of Liquid-Filled Projectiles under a Thrust", *Journal of Sound and Vibration*, Vol. 280, pp. 611–631, (2005).

[10] J. N. Reddy, *Theory and Analysis of Elastic Plates and Shells*, CRC Press, Taylor and Francis Group, New York, (2007).

[11] L. Meirovitch, *Analytical Methods in Vibrations*, The MacMillan Company, New York, (1967).

Table 1. Effect of axial vibration on n_{cr}.

h/R	*L/R* = 10		*L/R* = 20		*L/R* = 40		*L/R* = 60		*L/R* = 80		*L/R* = 100	
	B†	*C*††	*B*	*C*	*B*	*C*	*B*	*C*	*B*	*C*	*B*	*C*
0.01	5	5	4	4	3	3	3	3	2	2	2	2
0.03	3	3	3	3	2	2	2	2	2	2	2	1
0.05	3	3	2	2	2	2	2	2	2	2	1	1
0.075	3	3	2	2	2	2	2	2	1	1	1	1
0.1	2	2	2	2	2	2	1	1	1	1	1	1
0.125	2	2	2	2	1	1	1	1	1	1	1	1
0.15	2	2	2	2	1	1	1	1	1	1	1	1
0.175	2	2	2	2	1	1	1	1	1	1	1	1
0.2	2	2	2	2	1	1	1	1	1	1	1	1

†: Beck's problem; ††: Combined-effect problem

Table 2. η_C for different length and thickness ratios.

L/R / *h/R*	10	20	40	60	80	100
0.01	1.24	1.24	1.23	1.23	1.17	1.18
0.03	1.25	1.22	1.22	1.22	1.22	1.22
0.05	1.22	1.22	1.22	1.20	1.18	1.17
0.075	1.22	1.24	1.20	1.17	1.17	1.17
0.1	1.23	1.23	1.19	1.17	1.17	1.17
0.125	1.25	1.21	1.17	1.17	1.17	1.17
0.15	1.22	1.21	1.17	1.17	1.17	1.17
0.175	1.21	1.21	1.17	1.17	1.17	1.17
0.2	1.21	1.21	1.17	1.17	1.17	1.17

Appendix A

$$L_{11}=A_{11}\frac{\partial^2}{\partial x^2}+\left(\frac{A_{66}}{R^2}-\frac{1}{2}\frac{B_{66}}{R^3}\right)\frac{\partial^2}{\partial\theta^2}-I_0\frac{\partial^2}{\partial t^2},\ L_{12}=\left(\frac{A_{12}+A_{66}}{R}-\frac{1}{2}\frac{B_{66}}{R^2}\right)\frac{\partial^2}{\partial x\partial\theta},L_{13}=\frac{A_{12}}{R}\frac{\partial}{\partial x},\ L_{14}=B_{11}\frac{\partial^2}{\partial x^2}+\left(\frac{B_{66}}{R^2}-\frac{D_{66}}{R^3}\right)\frac{\partial^2}{\partial\theta^2}-I_1\frac{\partial^2}{\partial t^2},$$

$$L_{15}=\left(\frac{B_{12}+B_{66}}{R}-\frac{1}{2}\frac{D_{66}}{R^2}\right)\frac{\partial^2}{\partial x\partial\theta},L_{21}=\left(\frac{A_{12}+A_{66}}{R}+\frac{1}{2}\frac{B_{66}}{R^2}\right)\frac{\partial^2}{\partial x\partial\theta},\ L_{22}=-\bar{P}'(x)\frac{\partial}{\partial x}+\left(A_{66}+\frac{1}{2}\frac{B_{66}}{R}-\bar{P}(x)\right)\frac{\partial^2}{\partial x^2}+\frac{A_{22}}{R^2}\frac{\partial^2}{\partial\theta^2}-\frac{K_sA_{44}}{R^2}-I_0\frac{\partial^2}{\partial t^2},$$

$$L_{23}=\left(\frac{A_{22}}{R^2}+\frac{K_sA_{44}}{R^2}\right)\frac{\partial}{\partial\theta},\ L_{24}=\left(\frac{B_{12}+B_{66}}{R}+\frac{1}{2}\frac{D_{66}}{R^2}\right)\frac{\partial^2}{\partial x\partial\theta},\ L_{25}=\left(B_{66}+\frac{1}{2}\frac{D_{66}}{R}\right)\frac{\partial^2}{\partial x^2}+\frac{B_{22}}{R^2}\frac{\partial^2}{\partial\theta^2}+\frac{K_sA_{44}}{R}-I_1\frac{\partial^2}{\partial t^2},L_{31}=-L_{13},\ L_{32}=-L_{23},$$

$$L_{33}=-\bar{P}'(x)\frac{\partial}{\partial x}+\left(K_sA_{55}-\bar{P}(x)\right)\frac{\partial^2}{\partial x^2}-\frac{A_{22}}{R^2}+\frac{K_sA_{44}}{R^2}\frac{\partial^2}{\partial\theta^2}-I_0\frac{\partial^2}{\partial t^2},L_{34}=\left(-\frac{B_{12}}{R}+K_sA_{55}\right)\frac{\partial}{\partial x},\ L_{35}=\left(-\frac{B_{22}}{R^2}+\frac{K_sA_{44}}{R}\right)\frac{\partial}{\partial\theta},$$

$$L_{41}=B_{11}\frac{\partial^2}{\partial x^2}+\frac{B_{66}}{R^2}\frac{\partial^2}{\partial\theta^2}-I_1\frac{\partial^2}{\partial t^2},\ L_{42}=\left(\frac{B_{12}+B_{66}}{R}\right)\frac{\partial^2}{\partial x\partial\theta},\ L_{43}=-L_{34},L_{44}=-K_sA_{55}+D_{11}\frac{\partial^2}{\partial x^2}+\frac{D_{66}}{R^2}\frac{\partial^2}{\partial\theta^2}-I_2\frac{\partial^2}{\partial t^2},\ L_{45}=\left(\frac{D_{12}+D_{66}}{R}\right)\frac{\partial^2}{\partial x\partial\theta}$$

$$L_{51}=\left(\frac{B_{12}+B_{66}}{R}\right)\frac{\partial^2}{\partial x\partial\theta},\ L_{52}=B_{66}\frac{\partial^2}{\partial x^2}+\frac{B_{22}}{R^2}\frac{\partial^2}{\partial\theta^2}+\frac{K_sA_{44}}{R}-I_1\frac{\partial^2}{\partial t^2},\ L_{53}=-L_{35},L_{54}=L_{45},\ L_{55}=-K_sA_{44}+D_{66}\frac{\partial^2}{\partial x^2}+\frac{D_{22}}{R^2}\frac{\partial^2}{\partial\theta^2}-I_2\frac{\partial^2}{\partial t^2}$$

$$L'_{11}=-A_{11}\frac{\partial}{\partial x},\ L'_{12}=-\frac{A_{12}}{R}\frac{\partial}{\partial\theta},\ L'_{13}=-\frac{A_{12}}{R},\ L'_{14}=-B_{11}\frac{\partial}{\partial x},\ L'_{15}=-\frac{B_{12}}{R}\frac{\partial}{\partial\theta},L'_{21}=-\frac{A_{66}}{R}\frac{\partial}{\partial\theta},\ L'_{22}=A_{66}\frac{\partial}{\partial x},\ L'_{23}=0,\ L'_{24}=-\frac{B_{66}}{R}\frac{\partial}{\partial\theta},\ L'_{25}=-B_{66}\frac{\partial}{\partial x},$$

$$L'_{31}=L'_{32}=0,\ L'_{33}=-K_sA_{55}\frac{\partial}{\partial x},\ L'_{34}=-K_sA_{55},\ L'_{35}=0,L'_{41}=L'_{14},\ L'_{42}=-\frac{B_{12}}{R}\frac{\partial}{\partial\theta},\ L'_{43}=-\frac{B_{12}}{R},\ L'_{44}=-D_{11}\frac{\partial}{\partial x},\ L'_{45}=-\frac{D_{12}}{R}\frac{\partial}{\partial\theta},L'_{51}=-\frac{B_{66}}{R}\frac{\partial}{\partial\theta},$$

$$L'_{52}=L'_{25},\ L'_{53}=0,\ L'_{54}=-\frac{D_{66}}{R}\frac{\partial}{\partial\theta},\ L'_{55}=-D_{66}\frac{\partial}{\partial x}$$